Photoactive silicon surfaces functionalized with high-quality and redox-active platinum diimine complex monolayers

Bruno Fabre, Franck Camerel, Soraya Ababou-Girard

ARTICLE

Photoactive Silicon Surfaces Functionalized with High-Quality and Redox-Active Platinum Diimine Complexes Monolayers

Received 00th January 20xx,
Accepted 00th January 20xx

DOI: 10.1039/x0xx00000x

Bruno Fabre,*[a] Franck Camerel*[a] and Soraya Ababou-Girard[b]

New platinum diimine dichloro (**$PtCl_2$**) and dithiolene (**Ptdithiolene**) complexes have been synthesized and covalently bound to hydrogen-terminated, oxide-free silicon (111) surfaces using a two-step procedure. This immobilization route resulted in the formation of ca. 2.0-2.5 nm-thick densely packed and perfectly clean Pt complex monolayers with the expected structure of the grafted molecular chains. The surface coverages of attached **$PtCl_2$** and **Ptdithiolene** were electrochemically estimated at 8.9 x 10^{-11} and 7.5 x 10^{-11} mol.cm^{-2}, respectively, corresponding to 0.07 **$PtCl_2$** and 0.06 **Ptdithiolene** per surface silicon atom. The Pt complex-functionalized photoactive silicon surfaces showed under simulated sunlight a redox activity similar to that observed for the complexes in solution at a non-photoactive electrode. The two one-electron reduction processes centered on the bipyridine ligand were however observed at much less negative potentials, owing to the photovoltage generated at the silicon/monolayer interface. These modified photocathodes showed great promises for solar photoelectrocatalysis, as exemplified with the photoassisted electrocatalytic reduction of CO_2. Based on the measured cathodic photocurrent densities, the **Ptdithiolene**-modified surface showed superior catalytic performance.

1. Introduction

Well-defined platinum (Pt) complexes with polypyridine, vinylsiloxane, N-heterocyclic carbene or phosphine ligands have been widely used in very efficient and selective homogenous catalytic reactions.[1] A few attempts have been performed to immobilize these molecular systems on solid supports such as silica but it has not been established in all cases whether the catalytically active site is an isolated surface complex or a metal(0) aggregate.[2] Nevertheless, the immobilization of such complexes on photoactive semiconducting surfaces, such as silicon, appears us to be a promising strategy to elaborate light-activated functional devices. Surprisingly, only one example of a Pt molecular complex covalently grafted onto silicon has been reported so far and belongs to the family of heteroleptic Pt complexes, namely diimine-dithiolene complexes.

This intriguing class of complexes has been widely studied for their photophysical and redox properties. They have mainly been studied for their luminescence properties arising for the deactivation of a charge-transfer band between the diimine and the dithiolate fragments coordinated to the Pt center.[3] The proper choice of the diimine ligand and the dithiolate ligand allows the fine tuning of their photophysical and redox properties. Pt diimine-dithiolene complexes have been proposed as light harvester in the visible region for light-driven water reduction to hydrogen[4] but also in solar cells.[5] Crown ethers have been introduced on the dithiolate ligand in the [Pt(NN)(SS)] system for developing optical and electrochemical sensors for alkali metal cations.[6] It has also been demonstrated that the proper functionalization of the diimine or the dithiolate fragment with several long carbon chains or biphenyl fragments allows the complexes to self-organize into thermotropic liquid crystalline materials.[7] Recently, our group has indeed demonstrated that such metal complexes could be covalently attached on hydrogen-terminated silicon(100) surfaces through a hydrosilylation reaction with a dithiolate fragment ω–substituted with alkyne chains.[8] The so produced Si-C linked organometallic monolayers retained the redox activity of the Pt complexes exhibited in solution. Nevertheless, an oxidative decomposition of the grafted dithiolate ligand upon light exposure was observed impeding the photoelectrochemical investigation of the functional semiconducting surfaces.

Herein, the precursor structure has been judiciously revisited to avoid such light-induced degradation phenomenon. In particular, the unstable imino function present in the previously investigated Pt complexes has been eliminated in the present work because of its propensity to be hydrolyzed. Moreover, Si(111) surface was selected as the immobilization substrate preferentially to Si(100) which is extensively used in semiconductor technology. Indeed, it has been demonstrated that the organic functionalization of hydrogen-terminated

[a] *Univ Rennes, CNRS, ISCR (Institut des Sciences Chimiques de Rennes)-UMR6226, F-35000 Rennes, France.*
[b] *Univ Rennes, CNRS, IPR (Institut de Physique de Rennes)-UMR 6251, F-35000 Rennes, France.*

† Footnotes relating to the title and/or authors should appear here.

Electronic Supplementary Information (ESI) available: Details on the synthesis of the Pt complexes, their physicochemical characterizations, general instrumentation and DFT calculations; Details on the preparation of Pt complex-functionalized p-type Si(111) surfaces; Survey XPS spectra of the modified surfaces; Optimized geometrical structures of the Si(111)-bound Pt complexes; Additional electrochemical data; Determination of the surface coverages of the Pt complexes; Photothermal effect observed for the **Ptdithiolene** complex in solution. See DOI: 10.1039/x0xx00000x

Si(111) yielded usually both more densely packed and ordered monolayers, with a higher surface coverage.[9,10,11]

Two approaches have been tested to elaborate well-defined redox-active organometallic monolayers from the covalent derivatization of Si–H surfaces with Pt diimine-dithiolene complex. The first is based on the direct grafting of an alkene-terminated Pt diimine-dithiolene complex (denoted **Ptdithiolene** hereafter) onto Si–H through a hydrosilylation route (route a, Scheme 1). The second is a two-step method and consists first of a hydrosilylation reaction of di(dec-9-en-1-yl) [2,2'-bipyridine]-4,4'-dicarboxylate dichloro platinum complex (**$PtCl_2$**) with Si-H, followed by the conversion of the $PtCl_2$ moiety to the Pt diimine-dithiolene using a tin salt (route b, Scheme 1). In order to control both the quality, the composition and the compactness of the covalently bound organometallic monolayers, various experimental techniques have been used including cyclic voltammetry, X-ray photoelectron spectroscopy (XPS) and atomic force microscopy (AFM). Moreover, the promising catalytic effects exhibited by such complexes in solution for the electrochemical reduction of CO_2 prompted us to examine if such an activity was retained once immobilized on a photoactive surface.

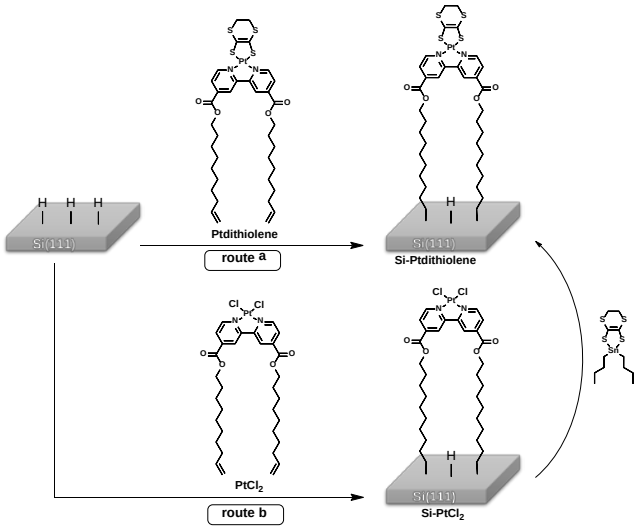

Scheme 1. Chemical Pathways for the Preparation of Pt Complex Monolayers Covalently Bound to Hydrogen-Terminated Si(111) Surfaces.

2. Results and Discussion.

2.1 Synthesis of Pt complexes.

An original bipyridine ligand carrying two long olefinic terminal chains has been developed for further grafting onto oxide-free Si(111) surfaces through a hydrosilylation reaction (see Scheme 1). The functional ligand was synthesized by reacting [2,2'-bipyridine]-4,4'-dicarboxylic acid chloride with 2.5 equivalents of 9-decen-1-ol in the presence of triethylamine. The synthesis of all the molecules and their principal physicochemical characterizations are fully described in the Supporting Information (Figures S1 to S5). The ligand was then reacted with 1 eq. of $PtCl_2(DMSO)_2$ to afford the corresponding dichloroplatinum diimine complexes **$PtCl_2$** in 80 % yield (Figures S6 to S11). Finally, the 5,6-dihydro-1,4-dithiin-2,3-dithiolato (dddt) ligand was introduced by a ligand metathesis by reacting the dichloroplatinum diimine complexes with one equivalent of 2,2-dibutyl-5,6-dihydro-1,3,2-dithiastannolo[4,5-b][1,4]dithiin in acetone to afford the corresponding diimine-dithiolene complexes **Ptdithiolene** as dark-green powders in 70 % yield (Figures S12 to S16). The purity and the molecular structure of all the compounds were confirmed by elemental analyses, ^{1}H NMR, ^{13}C NMR, mass spectrometry, IR spectroscopy and UV-vis analyses.

The UV-vis-NIR absorption spectra for all the compounds have been measured in CH_2Cl_2 solutions (Supporting Information). The absorption spectrum of the starting ligand showed two absorption bands with a maximum at 242 and 300 nm (Figure S3). These large absorption bands are assigned to π-π^* and n-π^* transitions localized on the bipyridine core.[12] After coordination by the $PtCl_2$ fragment, an additional absorption band with a weaker extinction coefficient appeared at 422 nm on the UV-vis spectrum of **$PtCl_2$** complex (Figure S8). This absorption band arises from a charge transfer transition from a filled Pt(d) orbital to an unoccupied π^* diimine orbital (MLCT).[13] Substitution of the chloride atoms by the $dddt^{2-}$ fragment in **Ptdithiolene** was characterized by the appearance of an intense absorption band at 774 nm (15700 M^{-1} cm^{-1}), associated to mixed metal ligand-to-ligand charge transfer transition (MMLL'CT) corresponding to excitation from the electron donor dithiolate ligand having orbital contributions from the metal ion to the electron acceptor bipyridine ligand (Figure S14).[7b, 14]

The thermal properties and stability of the ligand and associated metal complexes were also investigated upon repeated heating and cooling cycles by differential scanning calorimetry (DSC) and polarized optical microscopy (POM). The starting ligand melted around 63 °C and recrystallized with a strong supercooling around 20 °C (Figures S4 and S5). Upon cooling from the isotropic state, **$PtCl_2$** entered into a liquid crystalline state below 170 °C and characteristic textures of a columnar mesophase of hexagonal symmetry were observed by POM (Figures S9 and S10). The crystallization of this compound started below 70 °C. **Ptdithiolene** was in a liquid crystalline state from room temperature up to the degradation temperature at 140 °C (Figures S15 and S16) but no typical texture could have been developed. All the compounds were found to be stable up to 140 °C.

2.2 Electrochemical Properties of the Pt complexes and Electrocatalytic Activity for the CO_2 Reduction.

The electrochemical characteristics of the Pt complexes have been examined by cyclic voltammetry (CV) in CH_2Cl_2 medium, prior to their covalent immobilization on photoactive *p*-type Si(111) surfaces. In reduction and under argon, the CVs of **$PtCl_2$** and **Ptdithiolene** were characterized by two reversible waves at $E°'_{Red1}$ = -0.75 V and $E°'_{Red2}$ = -1.38 V vs Saturated Calomel Electrode (SCE) for **$PtCl_2$** and at $E°'_{Red1}$ = -0.88 V and $E°'_{Red2}$ = -1.48 V for **Ptdithiolene** (average of anodic and cathodic peak potentials). The reversible and monoelectronic character of both systems is supported by a peak-to-peak separation close to 60 mV (after Ohmic drop correction) and a ratio between the

anodic and cathodic peak current intensities close to 1 within the investigated potential scan range (i.e., 0.1-0.6 V s^{-1}). They correspond to the reduction of the neutral bipyridine ligand into its monoanionic and dianionic species, respectively.[8,15] Compared with **$PtCl_2$**, the reduction potentials of **Ptdithiolene** were slightly negatively shifted by 100-130 mV. Such a trend can be reasonably explained by the occurrence of a charge transfer between the dithiolate and the bipyridine ligands, as revealed by UV-visible measurements (*vide supra*), which renders the bipyridine fragment more electron rich and thus more difficult to reduce. An additional monoelectronic and reversible system was observed in oxidation at $E°'_{Ox}$ = +0.46 V only for **Ptdithiolene** and was attributed to the oxidation of the Pt dithiolate moiety to its radical cation form.[16]

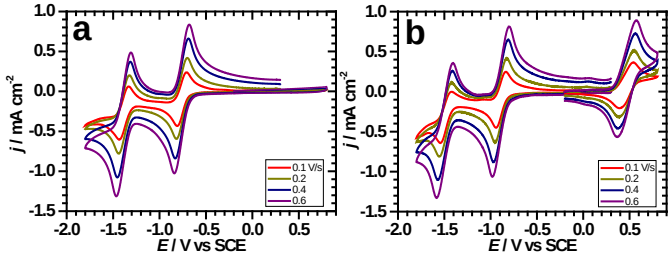

Figure 1. Cyclic voltammograms under argon of **$PtCl_2$** (a) and **Ptdithiolene** (b) at 2 mM in CH_2Cl_2 + 0.2 M Bu_4NPF_6 on glassy carbon (GC) electrode.

In a CO_2-saturated electrolyte solution, the CVs of **$PtCl_2$** and **Ptdithiolene** showed an increase in the cathodic current related to the second wave of the Pt complex whereas no significant current enhancement was observed in the absence of the Pt complex down to -1.8 V vs SCE (Figure 2). Such observations provide experimental evidence for the electrocatalytic activity of both Pt complexes towards the CO_2 reduction in homogeneous phase. Based on measured catalytic current densities, it cannot be however concluded that **Ptdithiolene** exhibits a higher activity than that of **$PtCl_2$**.

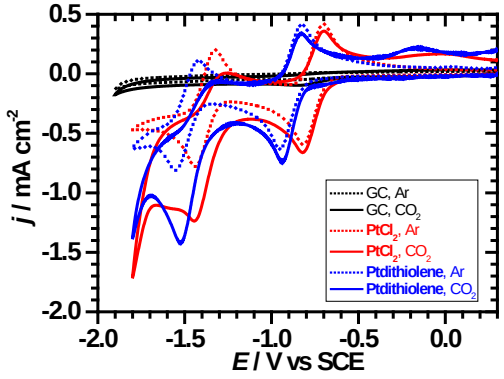

Figure 2. Comparative cyclic voltammograms at 0.2 V s^{-1} under argon (dotted lines) or CO_2 (solid lines) atmosphere of **$PtCl_2$** (red) and **Ptdithiolene** (blue) at 2 mM in CH_2Cl_2 + 0.2 M Bu_4NPF_6 on glassy carbon (GC) electrode. The black lines correspond to the electrochemical response of GC in the Pt complex-free electrolytic solution.

2.3 Covalent Grafting of Pt Complexes onto Photoactive Si(111) Surfaces.

The covalent derivatization of oxide-free, hydrogen-terminated Si(111) surfaces with Pt complexes was carried out following two grafting routes (Scheme 1). The first one based on the UV- or thermally-activated direct grafting of **Ptdithiolene** onto Si-H failed to produce high-quality and densely packed monolayers (see the Supporting Information for details and Table S1). Instead, an organometallic polymer film or a monolayer with low surface coverage (i.e. 3 x 10^{13} atoms cm^{-2}, i.e. 0.04 Pt complex per surface silicon atom) was deposited. In contrast, clean, high-quality and more densely packed Pt complex monolayers were produced from the two-step grafting consisting first of a hydrosilylation reaction at 300 nm of **$PtCl_2$** with Si-H, followed by the chemical conversion of the $PtCl_2$ moiety into a platinum-dithiolene moiety (route b, Scheme 1).

The composition of the optimized modified surfaces was determined by XPS. The survey spectra revealed characteristic peaks of the Si substrate itself (Si 2s and Si 2p), as well as characteristic signals of C 1s, Cl 2s, N 1s, S 2p, and Pt 4f, confirming the successful grafting of **$PtCl_2$** and **Ptdithiolene** (Figure S17). More specifically, for the $PtCl_2$-modified surface (denoted **Si-$PtCl_2$** hereafter), the high-resolution C 1s spectrum could be reasonably fitted using three components at 285.0, 286.7 and 289.4 eV, corresponding to different carbon atoms, namely [C-C + C=C], [CO + CN] and (C=O)O, respectively (Figure 3). The experimental ratios between the areas under the [C-C + C=C] and [CO + CN] peaks, and under the [CO + CN] and (C=O)O peaks, were estimated at 2.9 and 2.8, respectively, in relatively close agreement with the theoretical ratios of 4 (24:6) and 3 (6:2), respectively. The presence of Cl was supported by the presence of one peak at 269.4 eV on the Cl 2s signal and the area under the [C-C + C=C] and Cl peaks was also perfectly consistent with the expected ratio, 11.8 against 12 (24:2). Additionally, the N 1s signal showed a single component at 401.3 eV corresponding to nitrogen atoms of the bipyridine ligand, and the experimental atomic ratio between the total C and N was ca. 19.6 which is close to the expected ratio of 16 (32:2). The Pt 4f spectrum showed two components, the first one located at 72.7 eV (Pt $4f_{7/2}$) and 76.0 eV (Pt $4f_{5/2}$), and the second at 71.2 eV (Pt $4f_{7/2}$) and 74.9 eV (Pt $4f_{5/2}$). These are believed to correspond to two different geometrically Pt complex forms bound to the surface. From the approximate ratio, the contribution of the second minor component could be estimated at about 15% of total Pt.

After conversion of the **$PtCl_2$** to **Ptdithiolene**, no additional component was visible on the high-resolution C 1s spectrum of the **Ptdithiolene**-modified surface (**Si-Ptdithiolene**). We notice however that the second component attributed to heteroelement-bound carbon atoms (CO, CN and CS) was 0.3 eV-shifted towards lower binding energies. As expected, the replacement of the Cl atoms by the dithiolene unit was supported by the disappearance of the Cl 1s signal (indicating that the conversion was quantitative) and the emergence of a shoulder at approximately 162.6 eV on the plasmon loss peak of Si 2s corresponding to unresolved contributions of S $2p_{3/2}$ and $2p_{1/2}$ levels. The position of the N 1s peak was unchanged while the two components observed on the Pt 4f spectrum with their respective doublets were 0.4 eV-shifted to lower binding

energies compared with **Si-PtCl$_2$**. Such a shift would be rather consistent with a differently coordinated Pt complex, as previously reported for other organometallic monolayers bound to Si(111) surfaces.[17,18] The experimental ratio between the areas under the S 2p and N 1s peaks was estimated at 1.5, which is very close to 4S/2N expected for the terminal Pt complex. Finally, the chemical conversion of **PtCl$_2$** to **Ptdithiolene** was thought to indroduce some oxidation of the underlying silicon surface, as evidenced by the presence of a small peak at a binding energy of 103-104 eV attributable to silicon oxides.

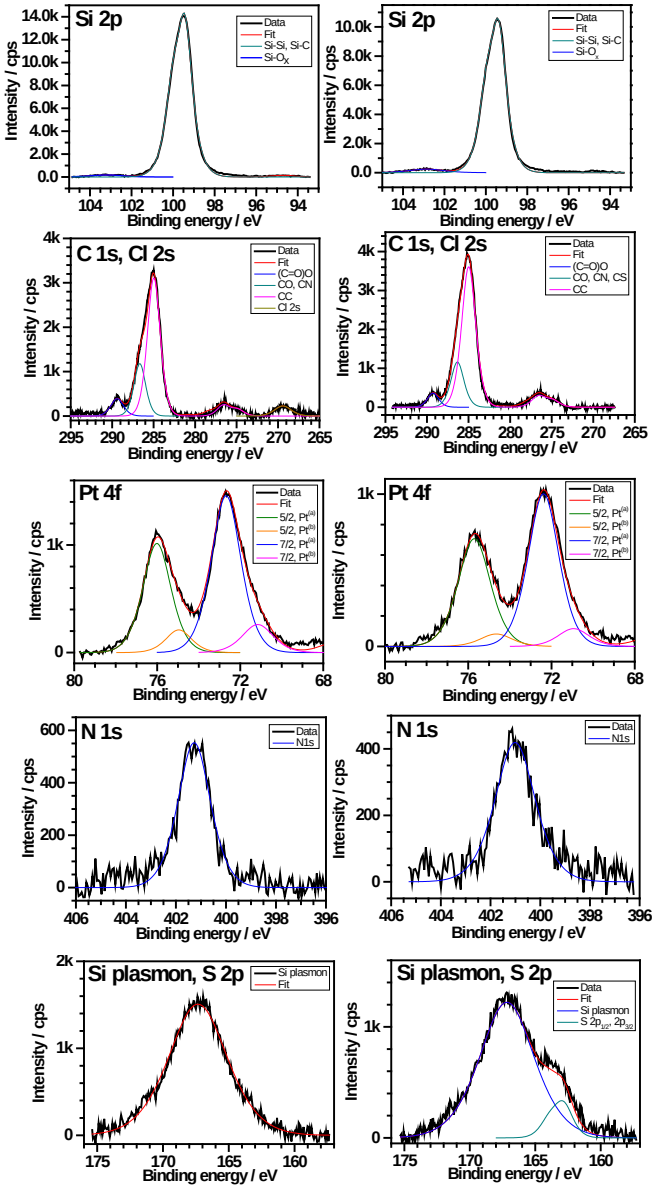

Figure 3. High-resolution XP spectra of Si 2p, C 1s and Cl 2s, Pt 4f, N 1s and S 2p for **Si-PtCl$_2$** (left column) and **Si-Ptdithiolene** (right column). The peak observed at about 276-277 eV on the C 1s spectra is attributed to satellite peaks of the used XPS source. Experimental data and fitting envelopes are represented by black and red lines, respectively. The colored lines are fitted curves using Gaussian–Lorentzian mixed peaks corresponding to different components.

Further characterization of the modified surfaces by spectroscopic ellipsometry yielded monolayer thicknesses of 19 ± 1 Å and 24 ± 1 Å for **Si-PtCl$_2$** and **Si-Ptdithiolene**, respectively. Such values were consistent with the theoretical lengths of the Pt complex-terminated molecular chains estimated at 21 ± 1 Å and 25.5 ± 1.5 Å for **Si-PtCl$_2$** and **Si-Ptdithiolene**, respectively, from Density Functional Theory (DFT) calculations (Figures S18 and S19).

The cleanliness of the optimized modified Si(111) surfaces was monitored by AFM. Both **Si-PtCl$_2$** and **Si-Ptdithiolene** showed a structure identical to that of Si(111)-H and other high-quality ω-functionalized organic monolayers,[19,20,21,22] with atomically flat, defect-free terraces separated by about 3 Å-high steps (Figure 4). Some oxidation pits were visible in the AFM image of **Si-Ptdithiolene** which were absent in that of **Si-PtCl$_2$**. The measured root-mean-square (rms) roughness was about 2 Å for both surfaces. Moreover, any contrast in friction images was not observed and any adventitious material was not removed upon a prolonged AFM tip scanning on the same place, thus providing experimental evidence that the surfaces were perfectly clean.

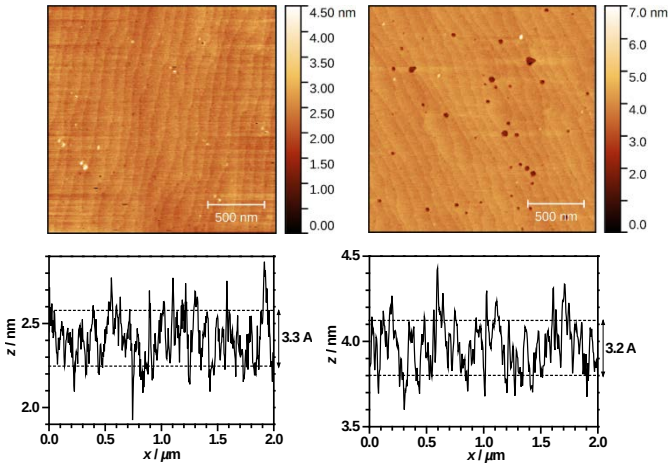

Figure 4. Tapping-mode AFM images (top) and corresponding cross-section profiles taken in the middle of the images (bottom) of **PtCl$_2$**- (left) and **Ptdithiolene**- (right) modified Si(111) surfaces.

2.4 Photoelectrochemical Properties of the Pt complex-Functionalized Silicon Photocathodes and Photoelectrocatalytic Activity for the CO_2 Reduction.

The electrochemical activity of the two Pt complex-functionalized silicon photocathodes has been examined in CH_3CN medium preferentially to CH_2Cl_2 used in homogeneous conditions owing to its higher electrical conductivity, its propensity to provide better resolved voltammetric peaks for redox monolayer-modified silicon surfaces[23] and the higher solubility of CO_2 in this solvent.[24] We have checked beforehand that the electrochemical behavior and the redox potentials of **PtCl$_2$** were quite similar in both solvents (Figure S21), **Ptdithiolene** having not been tested because of its poor solubility in CH_3CN. As shown in Figure 5, negligible current densities were measured in the dark for both **Si-PtCl$_2$** and **Si-**

Ptdithiolene surfaces. This situation is common for charge depleted semiconducting electrodes. Under these conditions, the concentration of majority charge carriers (i.e. holes) at the *p*-type silicon surface is not sufficient to promote the reduction processes assigned to the bipyridine ligand.[25] By contrast, much higher current densities were observed at illuminated modified silicon surfaces because the high concentration of photogenerated minority charge carriers (i.e. electrons) will promote efficiently the reduction processes. Importantly, due to the photogenerated electron-induced activation of the redox processes, the two reversible cathodic waves were observed at much less negative potentials than those determined at a non-photoactive electrode for the complexes in solution, namely $E°'_{Red1}$ = -0.65 V and $E°'_{Red2}$ = -1.03 V for **Si-PtCl$_2$** (Fig. 5a) and $E°'_{Red1}$ = -0.67 V and $E°'_{Red2}$ = -0.97 V for **Si-Ptdithiolene** (Fig. 5b). Such a potential shift called photovoltage is common for illuminated semiconducting photoelectrodes and is a desired characteristic for photoelectrocatalytic purposes.[26] It is worth however noting that the difference in formal potentials between the two redox processes ($E°'_{Red1} - E°'_{Red2}$) was much smaller for the immobilized systems than for the systems in solution. Such a trend could be ascribed to ion pairing effects with the electrolyte cation that may exist in solution but are most likely exacerbated for surface-attached electroactive molecules.[27] Another plausible explanation could be the presence of a strong carrier inversion layer in the semiconductor at the most negative potentials which would yield a higher photovoltage for the second redox process.[28]

Moreover, the total amount of Pt complexes attached to the surface was determined from the variation of cyclic voltammograms with the potential scan rate *v*. The cathodic peak photocurrent densities j_{pc} corresponding to the first redox process were found to be proportional to *v* within the range 0.0 −1.0 V s^{-1} (Figure S22), as expected for surface-confined redox species.[29] The slopes of the linear $j_{pc} - v$ plots yielded surface coverages of attached **PtCl$_2$** and **Ptdithiolene** of 8.9 x 10^{-11} and 7.5 x 10^{-11} mol cm^{-2}, respectively (see SI for details) which correspond to surface coverages of 0.07 **PtCl$_2$** and 0.06 **Ptdithiolene** per surface silicon atom, considering that the atomic density of Si(111) is 7.8 x 10^{14} atoms cm^{-2}.[30] Such values give specific areas of about 185 Å^2 per grafted **PtCl$_2$** and 220 Å^2 per grafted **Ptdithiolene**, which compare well with the theoretical specific areas determined from DFT calculations assuming that the two spacer arms of the grafted molecule are strongly spread on the surface, namely 184 Å^2 and 291 Å^2, respectively (Figure S18). At the opposite, these experimental values are somewhat greater than 118 Å^2 per grafted **PtCl$_2$** and 106 Å^2 per grafted **Ptdithiolene** by considering the two spacer arms of the molecule are closed together on the surface (Figure S19). Because the monolayer structure is probably between these two extreme cases, this indicates a reasonably dense packing of the Pt complex-terminated chains for both **Si-PtCl$_2$** and **Si-Ptdithiolene**. DFT calculations performed on monoanionic and dianionic species confirmed that the charge of the complex weakly affects the orientation and the conformation of the pendant aliphatic chains (Figure S20).

Now, the photoelectrocatalytic response of these functional surfaces was examined for the electrochemical reduction of CO_2. A clear enhancement in the cathodic photocurrent density was observed below -1.3 V vs SCE upon addition of CO_2 (Figure 6), in agreement with a catalytic activity of the modified photoelectrodes. The ratios between the cathodic photocurrent densities measured at -1.5 V in the presence (j_{cat}) and in the absence of CO_2 ($j°$) were estimated to be 3.1 and 6.6 for **Si-PtCl$_2$** and **Si-Ptdithiolene**, respectively, demonstrating the superior catalytic performance of **Ptdithiolene** in heterogeneous conditions. These preliminary results are promising and demonstrate that Pt diimine-dithiolene complexes show great potential for electrocatalytic applications.

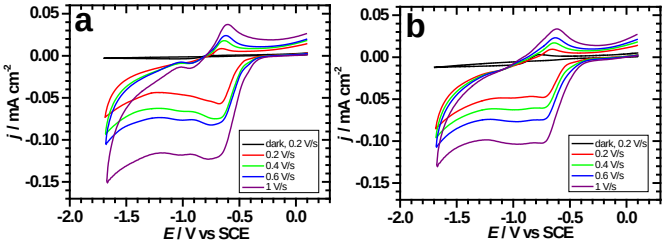

Figure 5. Ohmic drop-corrected CVs under illumination (AM 1.5G, 100 mW cm^{-2}) of **Si-PtCl$_2$** (a) and **Si-Ptdithiolene** (b) in CH_3CN + 0.1 M Bu_4NClO_4. The black traces correspond to the CVs in the dark at 0.2 V s^{-1}. *Details on the Ohmic drop correction method are provided in SI.*

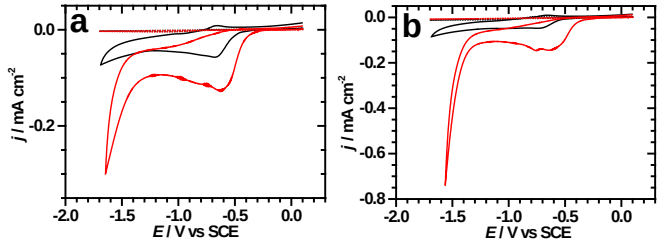

Figure 6. Ohmic drop-corrected CVs at 0.2 V s^{-1} in the dark (dotted lines) and under illumination (solid lines) of **Si-PtCl$_2$** (a) and **Si-Ptdithiolene** (b) under argon- (black) or CO_2- (red) saturated CH_3CN + 0.1 M Bu_4NClO_4 solution. *Details on the Ohmic drop correction method are provided in SI.*

3. Conclusions

In this work, we have demonstrated that platinum diimine complex monolayers could be covalently grafted onto oxide-free silicon(111) surfaces through a hydrosilylation reaction. Toward this goal, an original bipyridine ligand carrying two long carbon chains with a terminal alkene has been synthesized and the corresponding platinum complexes bearing chloride atoms and dithiolate fragment have been isolated. Both complexes displayed two reversible one-electron reduction processes centered on the bipyridine fragment. Cyclic voltammetry experiments performed in a CO_2-saturated electrolytic solution demonstrated that they exhibited an electrocatalytic activity towards the CO_2 reduction in homogeneous phase. Their covalent immobilization on oxide-free photoactive silicon surfaces was sequentially carried out by starting first by the grafting of the dichloro Pt complex followed by its chemical conversion to the diimine-dithiolene derivative. Such a strategy resulted in the formation of densely packed, clean and high-quality Pt complex monolayers, as supported by

electrochemistry, XPS, AFM and DFT geometry optimization calculations. The redox activity of both complexes was retained once immobilized but the two reversible cathodic waves were favorably shifted to less negative potentials thanks to the photogenerated electrons-induced activation of the redox processes. Both illuminated Pt complex-functionalized silicon photocathodes showed a photoelectrocatalytic activity towards the cathodic reduction of CO_2 but superior performance was observed for the **Ptdithiolene**-functionalized photocathode. Work is currently in progress in order to determine the performance metrics of these novel modified photoelectrodes and the selectivity of this catalytic reaction. The photothermal effect observed with the platinum diimine dithiolene complexes in solution could also be of great interest to boost the catalytic processes under laser irradiation in the NIR region.[31] Preliminary measurements have shown that the charge transfer **Ptdithiolene** complex, displaying a strong absorption band in the NIR region, could efficiently convert light under 808 nm laser irradiation with a photothermal efficiency around 29 % (Figure S23).[32]

Author Contributions

B. F. and F. C. designed the experiments, analyzed the data, and wrote the manuscript. S. A.-G. performed the XPS measurements. All authors have given approval to the final version of the manuscript.

Conflicts of interest

The authors declare no conflict of interest.

Acknowledgements

This work was granted access to the HPC resources of CINES under the allocation 2021-A0100805032 awarded by GENCI. Frédéric Barrière is gratefully acknowledged for his helpful discussion on DFT calculations. The authors thank Jean-François Bergamini for AFM experiments.

References

1 P. Ríos, A. Rodríguez and S. Conejero, *Chem. Commun.*, 2020, **56**, 5333-5349.
2 (a) M. Rimoldia and A. Mezzetti, *Catal. Sci. Technol.*, 2014, **4**, 2724-2740; (b) P. Laurent, L. Veyre, C. Thieuleux, S.Donet, C. Coperet, *Dalton Trans.*, 2013, **42**, 238-248.
3 (a) T. Kusamoto, S. Kume and H. Nishihara, *J. Am. Chem. Soc.*, 2008, **130**, 13844-13845; (b) W. Liu, R. Wang, X.-H. Zhou, J.-L. Zuo and X.-Z. You, *Organometallics*, 2008, **27**, 126-134; (c) W. Paw, S. D. Cummings, M. Adnan Mansour, W. B. Connick, D. K. Geiger and R. Eisenberg, *Coord. Chem. Rev.*, 1998, **171**, 125-150; (d) S. D. Cummings and R. Eisenberg, *Inorg. Chem.*, 1995, **34**, 2007-2014; (e) J. A. Zuleta, C. A. Chesta and R. Eisenberg, *J. Am. Chem. Soc.*, 1989, **111**, 8916-8917; (f) J. A. Zuleta, J. M. Bevilacqua, D. M. Proserpio, P. D. Harvey and R. Eisenberg, *Inorg. Chem.*, 1992, **31**, 2396-2404.
4 (a) J. Zhang, P. Du, J. Schneider, P. Jarosz and R. Eisenberg, *J. Am. Chem. Soc.*, 2007, **129**, 7726-7727; (b) G. Li, M. F. Mark, H. Lv, D. W. McCamant and R. Eisenberg, *J. Am. Chem. Soc.*, 2018, **140**, 2575-2586.
5 (a) B. W. Smucker, J. M. Hudson, M. A. Omary and K. R. Dunbar, *Inorg. Chem.*, 2003, **42**, 4714-4723; (b) K. Diwan, R. Chauhan, S. K. Singh, B. Singh, M. G. B. Drew, L. Bahadura and N. Singh, *New J. Chem.*, 2014, **38**, 97-108.
6 (a) Y. Ji, R. Zhang, X.-B. Du, J.-L. Zuo and X.-Z. You, *Dalton Trans.*, 2008, 2578-2582; (b) Y. Ji, R. Zhang, Y.-J. Li, Y.-Z. Li, J.-L. Zuo and X.-Z. You, *Inorg. Chem.*, 2007, **46**, 866-873.
7 (a) H.-C. Chang, K. Komasaka, K. Kishida, T. Shiozaki, T. Ohmori, T. Matsumoto, A. Kobayashi, M. Kato and S. Kitagawa, *Inorg. Chem.*, 2011, **50**, 4279–4288; (b) F. Camerel, G. Albert, F. Barrière, C. Lagrost, M. Fourmigué and O. Jeannin, *Chem. Eur. J.*, 2019, **25**, 5719-5732.
8 G. Yzambart, B. Fabre, T. Roisnel, V. Dorcet, S. Ababou-Girard, C. Meriadec and D. Lorcy, *Organometallics*, 2014, **33**, 4766–4776.
9 B. Fabre, *Acc. Chem. Res.*, 2010, **43**, 1509-1518.
10 S. Ciampi, J. B. Harper and J. J. Gooding, *Chem. Soc. Rev.*, 2010, **39**, 2158–2183.
11 J. M. Buriak, *Chem. Rev.*, 2002, **102**, 1271–1308.
12 C. E. Whittle, J. A. Weinstein, M. W. George and K. S. Schanze, *Inorg. Chem.*, 2001, **40**, 4053–4062.
13 (a) C.-W. Chan, L.-K. Cheng and C.-M. Che, *Coord. Chem. Rev.*, 1994, **132**, 87-97; (b) T. J. Wadas, R. J. Lachicotte and R. Eisenberg, *Inorg. Chem.*, 2003, **42**, 3772-3778; (c) V. M. Miskowski, V. H. Houlding, C.-M. Che, Y. Wang, *Inorg. Chem.*, 1993, **32**, 2518–2524.
14 (a) S. D. Cummings and R. Eisenberg, *J. Am. Chem. Soc.*, 1996, **118**, 1949-1960; (b) W. B. Connick and H. B. Gray, *J. Am. Chem. Soc.*, 1997, **119**, 11620-11627.
15 C. A. Mitsopoulou, *Coord. Chem. Rev.*, 2010, **254**, 1448–1456.
16 A. Vlcek, *Coord. Chem. Rev.*, 2009, **254**, 1357-1588.
17 K. Green, N. Gauthier, H. Sahnoune, J.-F. Halet, F. Paul and B. Fabre, *Organometallics*, 2013, **32**, 5333-5342.
18 G. Grelaud, N. Gauthier, Y. Luo, F. Paul, B. Fabre, F. Barrière, S. Ababou-Girard, T. Roisnel and M. G. Humphrey, *J. Phys. Chem. C*, 2014, **118**, 3680-3695.
19 D. Zigah, C. Herrier, L. Scheres, M. Giesbers, B. Fabre, P. Hapiot and H. Zuilhof, *Angew. Chem. Int. Ed.*, 2010, **49**, 3157-3160.
20 B. Fabre and F. Hauquier, *J. Phys. Chem. B*, 2006, **110**, 6848-6855.
21 L. C. P. M. de Smet, A. V. Pukin, Q.-Y. Sun, B. J. Eves, G. P. Lopinski, G. M. Visser, H. Zuilhof and E. J. R. Sudholter, *Appl. Surf. Sci.*, 2005, **252**, 24-30.
22 X. Wallart, C. H. de Villeneuve and P. Allongue, *J. Am. Chem. Soc.*, 2005, **127**, 7871-7878.
23 B. Fabre, *Chem. Rev.*, 2016, **116**, 4808-4849.
24 A. Gennaro, A. A. Isse and E. Vianello, *J. Electroanal. Chem.*, 1990, **289**, 203-215.
25 X. G. Zhang, Electrochemistry of silicon and its oxide, Kluwer Academic, New York, 2001.
26 S. Gimenez and J. Bisquert, Photoelectrochemical Solar Fuel Production: From Basic Principles to Advanced Devices, Springer, 2016.
27 D. H. Evans, *Chem. Rev.*, 2008, **108**, 2113-2144.
28 N. S. Lewis, *J. Electrochem. Soc.*, 1984, **131**, 2496-2503.
29 A. J. Bard and L. R. Faulkner, Electrochemical Methods. Fundamentals and Applications, Wiley, New York, 1980, p 522.
30 P. Allongue, C. Henry de Villeneuve and J. Pinson, *Electrochim. Acta*, 2000, **45**, 3241–3248.
31 L. Zhu, M. Gao, C. K. N. Peh, G. W. Ho, *Mater. Horiz.*, 2018, **5**, 323–343.
32 M. Ciancone, N. Bellec and F. Camerel, *ChemPhotoChem*, 2020, **4**, 5341–5345.

